Ke-Chang Hung and Jyh-Horng Wu*

Characteristics and thermal decomposition kinetics of wood-SiO_2 composites derived by the sol-gel process

DOI 10.1515/hf-2016-0126
Received August 12, 2016; accepted November 10, 2016; previously published online December 15, 2016

Abstract: Wood-SiO_2 composites ($WSiO_2Cs$) were prepared by means of the sol-gel process with methyltrimethoxysilane (MTMOS) as a reagent, and the physical properties, structure and thermal decomposition kinetics of the composites has been evaluated. The dimensional stability of the $WSiO_2Cs$ was better than that of unmodified wood, especially in terms of the weight percent gain (WPG), which achieved values up to 30%. The ^{29}Si-NMR spectra show two different siloxane peaks (T^2 and T^3), which supports the theory about the formation of MTMOS network structures. Thermal decomposition experiments were also carried out in a TG analyzer under a nitrogen atmosphere. The apparent activation energy was determined according to the iso-conversional methods of Friedman, Flynn-Wall-Ozawa, modified Coats-Redfern, and Starink. The apparent activation energy between 10 and 70% conversion is 147–172, 170–291, 189–251, and 192–248 kJ mol^{-1} for wood and $WSiO_2Cs$ with WPGs of 10, 20, and 30%, respectively. However, the reaction order between 10 and 70% conversion calculated by the Avrami theory was 0.50–0.56, 0.35–0.45, 0.33–0.44, and 0.28–0.48. These results indicate that the dimensional and thermal stability of the wood could be effectively enhanced by MTMOS treatment.

Keywords: activation energy, iso-conversion, methyltrimethoxysilane (MTMOS), reaction order, sol-gel process, thermal decomposition kinetics, thermal stability, wood-SiO_2 composites ($WSiO_2Cs$)

***Corresponding author: Jyh-Horng Wu,** Department of Forestry, National Chung Hsing University, Taichung 402, Taiwan, Phone: +886 4 22840345, Fax: +886 4 22851308, e-mail: eric@nchu.edu.tw
Ke-Chang Hung: Department of Forestry, National Chung Hsing University, Taichung 402, Taiwan

Introduction

Several wood modification techniques have been developed in the last decades to moderate the negative properties of wood such as dimensional instability under changing ambient humidity, biodeterioration, susceptibility to weathering and flammability. Acetylation, furfurylation (Moghaddam et al. 2016), treatment with inorganic materials (Zhang et al. 2016; Merk et al. 2016), heat treatment (Gao et al. 2016), and, more recently, the sol-gel technology receives a lot of attention (Hill 2006; Tshabalala et al. 2011; Shabir Mahr et al. 2012; Wang et al. 2012; Pries and Mai 2013; Gholamiyan et al. 2016; Mahr et al. 2016). The first wood-SiO_2 composite ($WSiO_2C$) prepared by the sol-gel process was performed by Saka et al. (1992). These type of composites are known to be effective in improving flame retardancy, UV stability, and fungal resistance (Kartal et al. 2004; Tshabalala et al. 2011; Qin and Zang 2012; Wang et al. 2012). Usually, the thermal stability of the sol-gel derived wood-inorganic composites is mostly estimated by thermal analyses, e.g. by differential scanning calorimetric (DSC) and thermogravimetric analyses (TGA) (Saka and Ueno 1997; Shabir Mahr et al. 2012; Wang et al. 2012). The activation energy is one of the most important parameters to describe the thermal decomposition behavior of the polymer materials and natural fibers (Yao et al. 2008; Poletto et al. 2012; Li et al. 2013). However, the effect of the sol-gel treatment on the activation energy of thermal decomposition of wood-inorganic composites has not yet been assessed.

On the other hand, "model-free" iso-conversion methods have been widely employed to determine the activation energy (E_a) of materials. These approaches allow the observation of the E_a dependence without assuming the reaction function and reaction order with the same conversion of the TG and DTG curves estimated at different heating rates (Yao et al. 2008; Gai et al. 2013). These models provide a quantitative evaluation of the thermal decomposition process and the stability of materials (Li et al. 2013) and provide reaction kinetics data over a broad temperature region (Gai et al. 2013). In this study, methyltrimethoxysilane (MTMOS) was used to prepare $WSiO_2Cs$,

and subsequently the thermal decomposition process of the composites with different SiO_2 solid contents has been investigated. Consequently, the E_a was evaluated via TGA by various model-free iso-conversional methods, including the methods of Friedman, Flynn-Wall-Ozawa (F-W-O), modified Coats-Redfern (modified C-R), and Starink (Yao et al. 2008; Gai et al. 2013). To the best of our knowledge, this is the first work addressing the thermal decomposition kinetics of wood-inorganic composites by the model-free iso-conversional methods.

Materials and methods

Materials: Japanese cedar (*Cryptomeria japonica* D. Don) sapwood (20–30 years old) was supplied by the experimental forest of the National Taiwan University. The dimensions of the slicewood samples were 3 mm (R)×12 mm (T)×58 mm (L). The oven-dried (o.d.) wood specimens selected for this study were free of defects and had a modulus of elasticity (MOE) from 8.0 to 9.0 GPa. The samples were investigated after extraction in a Soxhlet apparatus for 24 h with a 1 : 2 (v/v) mixture of ethanol and toluene, followed by washing with distilled water. The extracted slicewood was dried at 105°C for 12 h, and the o.d. weights were measured. The o.d. samples were conditioned at 20°C and 65% RH for 1 week before preparation of the $WSiO_2Cs$. MTMOS was purchased from Acros Chemical (Geel, Belgium). The other chemicals and solvents used in this experiment were of the highest quality available.

Preparation of wood-SiO_2 composites ($WSiO_2Cs$): The SiO_2-precursor sol was prepared with MTMOS, methanol, and acetic acid at a molar ratio of 0.12/1/0.005, 0.04, or 0.08 for preparing the $WSiO_2Cs$ with different weight percent gains (WPGs). The wood specimens were impregnated with the prepared sol under reduced pressure for 3 days. The impregnated specimens were then placed in an oven controlled to 50°C for 24 h and 105°C for another 24 h to age the gels (Miyafuji et al. 2004), and the WPG was calculated by the oven-dried method.

Determination of composite physical properties: The density, moisture content (MC), water absorption and volumetric swelling of the $WSiO_2Cs$ were determined according to the ASTM (D1037-06a 2006; D2395-07a 2007; D4442-07 2007) standards, respectively. The samples were conditioned at 20°C and 65% RH for 2 weeks before testing. The tests were repeated five times.

Attenuated total reflection-Fourier transform infrared (ATR-FTIR) spectroscopy: The spectra were recorded on a Spectrum 100 FTIR spectrometer (PerkinElmer, Buckinghamshire, UK) equipped with a DTGS detector and a MIRacle ATR accessory (Pike Technologies, USA). The spectra were collected by co-adding 32 scans at a resolution of 4 cm^{-1} in the range of 650 to 4000 cm^{-1}.

Solid-state CP/MAS ^{29}Si-NMR analysis: The powder samples were examined by the CP/MAS-^{29}Si-NMR technique. The spectra were recorded on a Bruker DSX-400WB FT-NMR spectrometer (Bremen, Germany) with a sampling frequency of 80 MHz. The chemical shifts were calculated relative to tetramethylsilane (TMS).

Thermogravimetric analysis (TGA): A PerkinElmer Pyris 1 TG analyzer (Shelton, USA) was used. Measurements of 3 mg samples were carried out in a nitrogen atmosphere (20 ml min^{-1}) from 50 to 600°C. The heating rate was set to 5, 10, 20, 30, and 40°C min^{-1}. The kinetic parameters were calculated based on the data obtained by the model free iso-conversional methods. The conversion rate α is defined as:

$$\alpha = (W_0 - W_t)/(W_0 - W_\infty) \quad (1)$$

where W_0 is the initial weight of the sample, W_∞ is the final residual weight, and W_t is the weight of the oxidized or pyrolized sample at time t. The common iso-conversional methods used in this study include the methods of Friedman (Eq. 2), F-W-O (Eq. 3), modified C-R (Eq. 4), and Starink (Eq. 5). The methods are represented by the following equations:

$$\ln(d\alpha/dt) = \ln[Af(\alpha)] - E_a/(RT) \quad (2)$$

$$\log\beta = \log[AE_a/(Rg(\alpha))] - 2.315 - 0.4567E_a/(RT) \quad (3)$$

$$\ln\{\beta/[T^2(1-2RT/E_a)]\} = \ln\{-AR/[E_a\ln(1-\alpha)]\} - E_a/(RT) \quad (4)$$

$$\ln(\beta/T^{1.8}) = C_s - 1.0037(E_a/RT) \quad (5)$$

where α is the conversion rate, A is the pre-exponential factor (min^{-1}), $f(\alpha)$ is the reaction model, E_a is the apparent E_a (kJ mol^{-1}), R is the gas constant (8.314 J K^{-1} mol^{-1}), T is the absolute temperature (K), β is the heating rate, $g(\alpha)$ is a function of the conversion, and C_s is a constant (Yao et al. 2008; Gai et al. 2013; Li et al. 2013). Therefore, for a given conversion, linear relationships are observed by plotting $\ln(d\alpha/dt)$, $\log\beta$, $\ln(\beta/T^2)$, and $\ln(\beta/T^{1.8})$ vs. $1/T$ at different heating rates; the E_a is calculated from the slope of the straight line (Yao et al. 2008; Gai et al. 2013; Li et al. 2013).

In addition to E_a, the reaction order is also an important parameter for the thermal decomposition of wood (Gai et al. 2013). Reaction order in this study was calculated based on the Avrami theory (Eq. 6):

$$\ln[-\ln(1-\alpha)] = \ln A - E_a/RT - n\ln\beta \quad (6)$$

where n represents the reaction order. For a given temperature, a linear relationship is observed by plotting $\ln[-\ln(1-\alpha)]$ vs. $\ln\beta$ at different temperature heating rates, and the reaction order is deduced from the slope of the line (Gai et al. 2013).

Analysis of variance: All results were expressed in terms of the mean ± SD. The significance of the differences were calculated by the Scheffe's test; P values < 0.05 were considered to be significant.

Results and discussion

Physical properties of $WSiO_2Cs$

The various physical properties of $WSiO_2Cs$ with different WPGs are listed in Table 1. Accordingly, the density of all samples ranged between 437 and 507 kg m^{-3}, and the MC of the samples decreased with increasing WPG. In addition, after 24 h of water immersion, the water absorption

Table 1: Physical properties of wood and wood-SiO_2 composites.

Specimen	WPG (%)	Density (kg m^{-3})	Moisture content (%)	24 h soaking	
				Water absorption (%)	Volume swelling (%)
Wood	0	437 ± 17^{b}	9.42 ± 0.31^{a}	100 ± 17^{a}	10.4 ± 2.8^{a}
Wood-SiO_2 composites	10	507 ± 18^{a}	8.68 ± 0.04^{b}	54 ± 3^{b}	4.4 ± 0.6^{b}
	20	442 ± 14^{b}	7.77 ± 0.22^{c}	34 ± 3^{c}	3.3 ± 0.9^{b}
	30	467 ± 34^{a,b}	7.32 ± 0.18^{d}	26 ± 3^{c}	2.0 ± 0.7^{b}

Values are the means ± SD (n = 5). Different superscript letters within a column indicate significant difference at $P < 0.05$.

and volume swelling of the $WSiO_2Cs$ were significantly different from the untreated wood (W). The W had the highest volume swelling (10.4%) and water absorption (100%). In contrast, all of the $WSiO_2Cs$ exhibit excellent data with volume swelling between 2.0 and 4.4%, and water absorption between 26 and 54%. Among the samples, the $WSiO_2C$ with a WPG of 30% revealed the best data due to the reaction of silicon compounds because of an effective hydrophobication and bulking of the cell wall (Kartal et al. 2009; Tshabalala et al. 2011; Wang et al. 2012). Clearly, only the deposition of reactive agents in the cell wall is effective; those in the cell lumen play only a minor role (Wang et al. 2012). Therefore, it can be concluded that $WSiO_2Cs$ with WPGs between 20 and 30% are probably deposited in the cell wall. Beginning with a WPG of 30%, more and more $WSiO_2C$ is deposited also in the cell lumen.

Chemical structure of $WSiO_2Cs$

The characteristics of wood before and after MTMOS treatment was elucidated by FTIR and CP/MAS ^{29}Si-NMR. The FTIR spectra of W and $WSiO_2Cs$ with different WPGs are illustrated in Figure 1a. After MTMOS treatment, the absorption band at 1270 (Si-CH_3, ν), 1104 (Si-O-Si, δ), 1031 (Si-O-Si, δ), 900 (Si-O-C, ν), and 778 cm^{-1} (Si-O-C, ν) increased in all composites (Tshabalala and Sung 2007; Ghosh et al. 2009). Among those, the Si-O-Si group can be attributed to the condensation reaction of MTMOS with dehydration or dealcoholization (Chiang and Ma 2004). This result confirms that the $WSiO_2Cs$ have a specific silica (SiO_2) band and supports the hypothesis that silica is within the cell wall, all the more as these absorption bands also increased significantly with increasing WPGs.

Figure 1b presents the solid-state ^{29}Si-NMR spectra of the W and $WSiO_2Cs$. Any characteristic signals are absent in the W. Three peaks are visible in the $WSiO_2Cs$ with chemical shifts of −46 (T^1), −55 (T^2), and −65 (T^3) ppm,

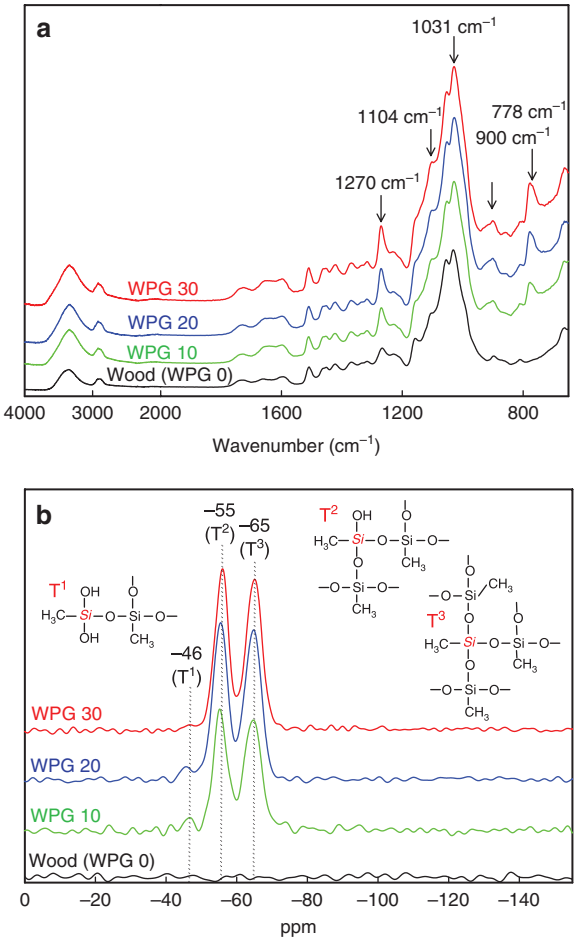

Figure 1: FTIR spectra (a) and solid-state ^{29}Si NMR spectra (b) of wood and wood-SiO_2 composites with different WPGs.

which are assigned to the MTMOS with mono-, di-, and tri-substituted siloxane bonds (Joseph et al. 1996; Chiang and Ma 2004). This is again a hint that silica mixtures are formed in the composites. The signal intensities of T^2 and T^3 are more pronounced for all $WSiO_2Cs$, thus these signals play the largest role in the $WSiO_2Cs$. Accordingly, the condensation degree of siloxane is high, and the MTMOS formed a network structure in the composite in the course of the sol-gel process.

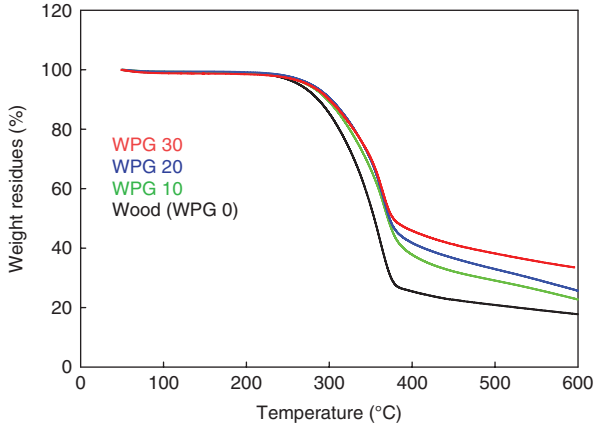

Figure 2: Thermogravimetric curves of wood and wood-SiO_2 composites with different WPGs.

Thermal properties of $WSiO_2Cs$

Figure 2 shows the TGA curves of W and $WSiO_2Cs$. The W-TGA curve indicates a gradually increasing weight loss (WL) above 200°C. This effect is well known (Fengel and Wegener 1989). A maximum WL was obtained around 350°C, which is due to the pyrolysis of the wood components among which the hemicelluloses are the less stable (Boonstra and Tjeerdsma 2006; Chaouch et al. 2010; Wang et al. 2012). The pyrolysis of the $WSiO_2Cs$ was by ca. 10°C delayed compared to W. Saka and Ueno (1997) and Miyafuji and Saka (2001) made similar observations. The solid residue left at 600°C was in case of $WSiO_2Cs$ higher than for W (17.9%). The higher of the WPG of the $WSiO_2Cs$, the more solid char was left at 600°C ($WPG_{10\%}$ 23.1% char; $WPG_{30\%}$ 33.6% char) because of the higher amount of the deposited inorganic SiO_2. Of course, it is also possible that the deposited SiO_2 additionally increased the yield of the wood based charcoal (Rowell and LeVan-Green 2005). Obviously, the $WSiO_2Cs$ are more thermally stable as decomposition temperatures shifted to the region of higher temperature and the solid residues also increased (Li et al. 2013).

For an in-depth process analysis, the model free iso-conversional methods were applied for TG data evaluation. The plots of the iso-conversional Friedman, F-W-O, modified C-R, and Starink methods depict a general trend in the E_a. As an example, typical plots based on the models F-W-O, modified C-R, Friedman, and Starink for W are presented in Figure 3. The slopes of the fitted lines between 10 and 70% conversion were nearly parallel, indicating the approximate E_a at different conversion methods. The $WSiO_2Cs$ plots are similar to those presented in Figure 3 (not shown). As suggested by Yao et al. (2008), a single

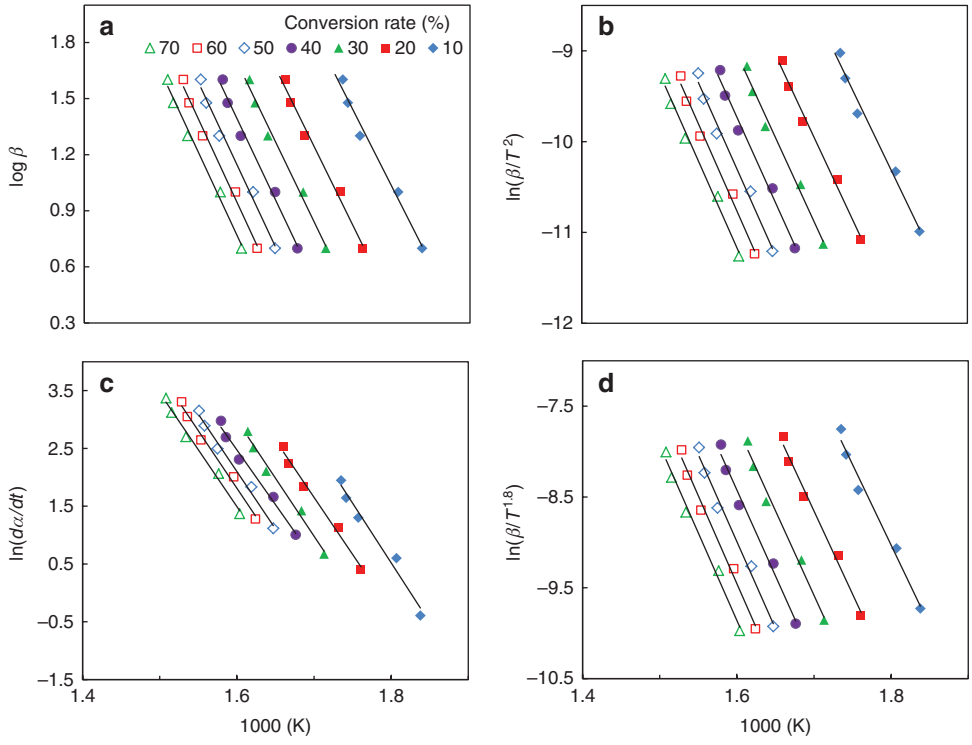

Figure 3: Typical iso-conversional plots of F-W-O (a), modified C-R (b), Friedman (c), and Starink (d) methods for wood.

Table 2: Apparent activation energy and reaction order of wood and wood-SiO_2 composites ($WSiO_2Cs$) calculated by the F-W-O, modified C-R, Friedmann, Starink methods, and Avrami theory.

		Conversion rates							
Material/methods	**Units**	**10%**	**20%**	**30%**	**40%**	**50%**	**60%**	**70%**	**Mean**
Wood	E_a (kJ mol^{-1})	148	153	156	159	160	162	162	157
F-W-O	R^2	0.983	0.988	0.988	0.987	0.989	0.990	0.990	–
Wood	E_a (kJ mol^{-1})	147	151	154	157	158	160	160	155
Modified C-R	R^2	0.981	0.987	0.986	0.986	0.987	0.989	0.989	–
Wood	E_a (kJ mol^{-1})	172	164	167	158	165	165	164	165
Friedmann	R^2	0.973	0.989	0.986	0.986	0.988	0.998	0.989	–
Wood	E_a (kJ mol^{-1})	147	152	154	157	159	160	160	156
Starink	R^2	0.981	0.987	0.986	0.986	0.987	0.989	0.989	–
Wood	Reac. order	0.52	0.52	0.51	0.50	0.50	0.52	0.56	0.52
Avrami theory	R^2	0.980	0.984	0.985	0.987	0.987	0.985	0.986	–
W/SiO_2 10%	E_a (kJ mol^{-1})	190	186	189	192	190	192	214	193
F-W-O	R^2	0.994	0.999	0.999	0.999	0.998	0.998	≈ 1	–
W/SiO_2 10%	E_a (kJ mol^{-1})	190	186	189	192	189	191	215	193
Modified C-R	R^2	0.993	0.999	0.999	0.999	0.998	0.998	≈ 1	–
W/SiO_2 10%	E_a (kJ mol^{-1})	170	204	189	195	180	202	291	204
Friedmann	R^2	0.978	0.995	0.996	0.994	0.990	0.998	0.994	–
W/SiO_2 10%	E_a (kJ mol^{-1})	190	186	189	192	190	191	215	193
Starink	R^2	0.993	0.999	0.999	0.999	0.998	0.998	≈ 1	–
W/SiO_2 10%	Reac. order	0.35	0.41	0.40	0.39	0.40	0.43	0.45	0.40
Avrami theory	R^2	0.978	0.996	0.999	≈ 1	0.997	0.992	0.998	–
W/SiO_2 20%	E_a (kJ mol^{-1})	196	189	201	205	204	200	210	201
F-W-O	R^2	0.995	0.997	0.997	0.997	0.999	0.998	0.998	–
W/SiO_2 20%	E_a (kJ mol^{-1})	197	198	201	205	204	199	210	201
Modified C-R	R^2	0.994	0.996	0.997	0.997	0.999	0.998	0.998	–
W/SiO_2 20%	E_a (kJ mol^{-1})	195	208	220	200	221	203	251	214
Friedmann	R^2	0.992	0.983	0.992	0.994	0.997	0.999	0.985	–
W/SiO_2 20%	E_a (kJmol^{-1})	197	198	201	205	204	200	210	202
Satrink	R^2	0.994	0.997	0.997	0.997	0.999	0.998	0.998	–
W/SiO_2 20%	Reac. order	0.33	0.38	0.37	0.36	0.37	0.41	0.44	0.38
Avrami theory	R^2	0.991	0.997	0.994	0.996	0.997	0.994	0.998	–
W/SiO_2 30%	E_a (kJ mol^{-1})	245	214	215	212	204	199	198	212
F-W-O	R^2	0.972	0.995	0.997	0.998	0.999	0.999	0.999	–
W/SiO_2 30%	E_a (kJ mol^{-1})	248	215	216	212	204	198	197	213
Modified C-R	R^2	0.970	0.994	0.997	0.998	0.999	0.999	0.999	–
W/SiO_2 30%	E_a (kJ mol^{-1})	237	209	219	206	194	192	203	209
Friedmann	R^2	0.985	0.967	0.998	0.999	0.998	0.999	0.999	–
W/SiO_2 30%	E_a (kJ mol^{-1})	248	216	216	213	204	199	197	213
Starink	R^2	0.970	0.994	0.997	0.998	0.999	0.999	0.999	–
W/SiO_2 30%	Reac. order	0.28	0.35	0.36	0.35	0.37	0.42	0.48	0.37
Avrami theory	R^2	0.887	0.988	0.997	0.997	0.992	0.981	0.976	–

possible reaction mechanism takes place between 10 and 70% conversion in natural fibers. Therefore, in this study, the apparent E_a was estimated in this conversion range. The correlation coefficient (R^2) and the E_a values calculated from the above mentioned methods are listed in Table 2.

As seen in Table 2, the E_a values of W are between 148 and 162 kJ mol^{-1} (at the conversion range 10 to 70%), and the E_a value increases with increasing conversion rate. As found by Yao et al. (2008), the average apparent E_a of maple and pine calculated between 10 and 60% by the F-W-O method was 155.8 and 161.8 kJ mol^{-1}, respectively. In the present study, the average apparent E_a of wood is 157 kJ mol^{-1}, which is in good agreement with literature data. Moreover, the average apparent E_a of the $WSiO_2Cs$ was 193, 201, and 212 kJ mol^{-1} for WPGs of 10, 20, and 30%, respectively. The E_a is defined as the minimum energy that must be overcome to start a chemical reaction (Gao et al. 2016). As the E_a values increased with increasing WPG of

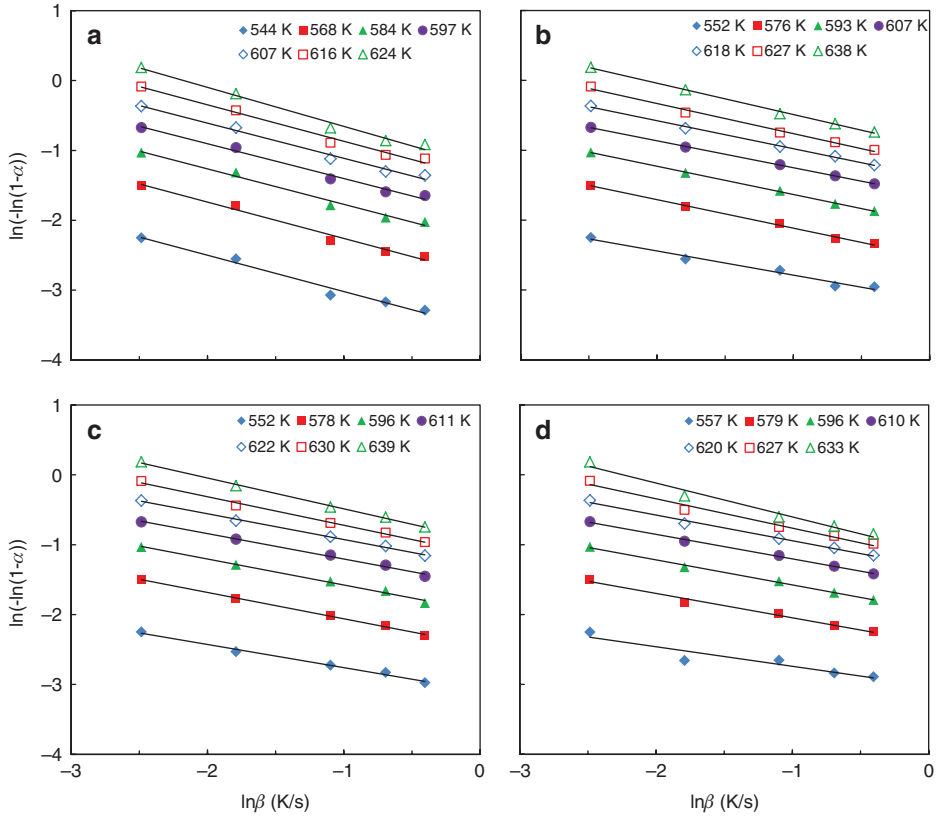

Figure 4: Regression lines to reaction order proposed by Avrami theory for wood (a) and wood-SiO_2 composites with WPGs of 10% (b), 20% (c), and 30% (d).

the $WSiO_2Cs$, the minimum energy required to start the thermal decomposition was also elevated. One possible explanation is that incorporation of silica into the wood forms a closed barrier layer and effectively shielded the wood components from being accessible to air and thus retarding their combustion (Miyafuji and Saka 1997; Wang et al. 2012).

As further shown in Table 2, similar results from modified C-R, Friedman, and Starink methods also confirm this observation. The average E_a values calculated in the conversion range of 10–70% were 155–165, 193–204, 201–214, and 209–213 kJ mol^{-1} for W and $WSiO_2Cs$ with WPGs of 10, 20, and 30%, respectively. The variation of the average E_a values by the Friedman method was greater than that calculated by the other three methods for the $WSiO_2Cs$ with WPGs of 10 and 20%. The E_a at 70% conversion was especially high. A statement of Brown et al. (2000) and Yao et al. (2008) should remembered, according to which different kinetic analysis methods are complementary rather than competitive. Thus, a suitable apparent E_a range could be obtained by combining all observations in Table 2. Consequently, an E_a range of 147–172, 170–291, 189–251, and 192–248 kJ mol^{-1} is valid for W and $WSiO_2Cs$ with WPGs of 10, 20, and 30%, respectively. This E_a range is similar to that reported by Yao et al. (2008).

To estimate the dependence of the reaction order (n) on the decomposition temperature during the major thermal decomposition process, seven decomposition temperatures were employed at five heating rates (5, 10, 20, 30, and 40 K min^{-1}). The seven decomposition temperatures were the temperature of conversion between 10 and 70% at a heating rate of 5 K min^{-1}. Based on the Avrami theory, the regression lines of the W and $WSiO_2Cs$ are illustrated in Figure 4. The calculated reaction order and corresponding R^2 values are also presented in Table 2. It is remarkable that most R^2 values are higher than 0.99. Thus, the Avrami theory is suitable to evaluate the reaction order of W and $WSiO_2Cs$. The reaction order ranged 0.50–0.56, 0.35–0.45, 0.33–0.44, and 0.28–0.48 for W and $WSiO_2Cs$ with WPGs of 10, 20, and 30%, respectively (Table 2). The reaction order of wood waste is 0.42 (Vuthaluru 2004), and those of corn straw and rice husks are 0.365 and 0.539, respectively (Gai et al. 2013). Interestingly, the mean value of the reaction orders of the W and $WSiO_2Cs$ display an opposite trend as the reaction energy. The reaction order of specimen generally decreased with

increasing WPG of the $WSiO_2C$, thus the SiO_2 in the wood may have changed the thermal decomposition path. The SiO_2 could have reduced the combustible volatiles and formed a closed barrier layer, which retards the pyrolysis or combustion process. No doubt, the MTMOS treatment improves the thermal stability.

Conclusions

Japanese cedar slicewood was used to prepare $WSiO_2Cs$ by the sol-gel process with MTMOS. The thermal decomposition process of the specimens was observed by dynamic TG analysis and from the data apparent activation energy (E_a) data were calculated. These results indicate that the incorporation of SiO_2 into the wood cell wall significantly reduced the moisture sorption and hydrophilicity of wood. Consequently, the dimensional stability, especially at a high WPG, was improved. According to the FTIR and CP/MAS ^{29}Si-NMR spectra, the silica was formed from the composites, and the T^2 and T^3 signals were the major indicators of the $WSiO_2C$. The TG curves of the $WSiO_2Cs$ shifted to a higher temperature field compared to the untreated wood. The average apparent E_a of the $WSiO_2Cs$ was higher than that of the untreated wood and increased with increasing WPGs, up to 30%. For the range of conversion rates (10–70%) investigated, the reaction order was 0.50–0.56, 0.35–0.45, 0.33–0.44, and 0.28–0.48 for wood and $WSiO_2Cs$ with WPGs of 10, 20, and 30%, respectively. These results indicate that the wood could be functionalized with MTMOS to obtain wood with enhanced dimensional and thermal stability.

Acknowledgements: This work was financially supported by a research grant from the Ministry of Science and Technology, Taiwan (NSC 102-2628-B-005-006-MY3).

References

ASTM D1037-06a (2006) Standard test methods for evaluating properties of wood-based fiber and particle panel materials. ASTM International, West Conshohocken, PA.

ASTM D2395-07a (2007) Standard test methods for specific gravity of wood and wood-based materials. ASTM International, West Conshohocken, PA.

ASTM D4442-07 (2007) Standard test methods for direct moisture content measurement of wood and wood-based materials. ASTM International, West Conshohocken, PA.

Boonstra, M.J., Tjeerdsma, B. (2006) Chemical analysis of heat treated softwoods. Eur. J. Wood Prod. 64:204–211.

Brown, M.E., Maciejewski, M., Vyazovkin, S., Nomen, R. Sempere, J., Burnham, A. (2000) Computational aspects of kinetic analysis. Part A: the ICTAC kinetics project-data, methods and results. Thermochim. Acta 355:125–143.

Chaouch, M., Pétrissans, M., Pétrissans, A., Gérardin, P. (2010) Use of wood elemental composition to predict heat treatment intensity and decay resistance of different softwood and hardwood species. Polym. Degrad. Stabil. 95:2255–2259.

Chiang, C.-L., Ma, C.-C.M. (2004) Synthesis, characterization, thermal properties and flame retardance of novel phenolic resin/silica nanocomposites. Polym. Degrad. Stabil. 83:207–214.

Fengel, D., Wegener, G. Wood: Chemistry, Ultrastructure, Reaction. Walter de Gruyter, Berlin, 1989.

Gai, C., Dong, Y., Zhang, T. (2013) The kinetic analysis of the pyrolysis of agricultural residue under non-isothermal conditions. Bioresource Technol. 127:298–305.

Gao, J., Kim, J.S., Terziev, N., Daniel, G. (2016) Decay resistance of softwoods and hardwoods thermally modified by the thermovouto type thermo-vacuum process to brown rot and white rot fungi. Holzforschung 70:877–884.

Gholamiyan, H., Tarmian, A., Ranjbar, Z., Abdulkhani, A., Azadfallah, M., Mai, C. (2016) Silane nanofilm formation by sol-gel processes for promoting adhesion of waterborne and solventborne coatings to wood surface. Holzforschung 70:429–437.

Ghosh, S.C., Militz, H., Mai, C. (2009) The efficacy of commercial silicones against blue stain and mould fungi in wood. Eur. J. Wood Prod. 67:159–167.

Hill, C.A.S. Wood Modification: Chemical, Thermal and Other Processes. John Wiley & Sons, Chichester, 2006.

Joseph, R., Zhang, S., Ford, W.T. (1996) Structure and dynamics of a colloidal silica-poly(methyl methacrylate) composite by ^{13}C and ^{29}Si MAS NMR spectroscopy. Macromolecules 29:1305–1312.

Kartal, S.N., Yoshimura, T., Imamura, Y. (2004) Decay and termite resistance of boron-treated and chemically modified wood by in situ co-polymerization of allyl glycidyl ether (AGE) with methyl methacrylate (MMA). Int. Biodeterior. Biodegrad. 53:111–117.

Kartal, S.N., Yoshimura, T., Imamura, Y. (2009) Modification of wood with Si compounds to limit boron leaching from treated wood and to increase termite and decay resistance. Int. Biodeterior. Biodegrad. 63:187–190.

Li, Y., Du, L., Kai, C., Huang, R., Wu, Q. (2013) Bamboo and high density polyethylene composite with heat-treated bamboo fiber: thermal decomposition properties. Bioresources 8:900–912.

Mahr, M.S., Hübert, T., Stephan, I., Bücker, M., Militz, H. (2016) Reducing copper leaching from treated wood by sol-gel derived TiO_2 and SiO_2 depositions. Holzforschung 67:429–435.

Merk, V., Chanana, M., Gaan, S., Burgert, I. (2016) Mineralization of wood by calcium carbonate insertion for improved flame retardancy. Holzforschung 70:867–876.

Miyafuji, H., Kokaji, H., Saka, S. (2004) Photostable wood-inorganic composites prepared by the sol-gel process with UV absorbent. J. Wood Sci. 50:130–135.

Miyafuji, H., Saka, S. (1997) Fire-resistant properties in several TiO_2 wood-inorganic composites and their topochemistry. Wood Sci. Technol. 31:449–455.

Miyafuji, H., Saka, S. (2001) Na_2O-SiO_2 wood-inorganic composites prepared by the sol-gel process and their fire-resistant properties. J. Wood Sci. 47:483–489.

Moghaddam, M.S., Wålinder, M.E.P., Claesson, P.M., Swerin, A. (2016) Wettability and swelling of acetylated and furfu-

rylated wood analyzed by multicycle Wilhelmy plate method. Holzforschung 70:69–77.

Poletto, M., Zattera, A.J., Santana, R.M.C. (2012) Thermal decomposition of wood: kinetics and degradation mechanisms. Bioresource Technol. 126:7–12.

Pries, M., Mai, C. (2013) Fire resistance of wood treated with a cationic silica sol. Eur. J. Wood Prod. 71:237–244.

Qin, C., Zang, W. (2012) Antibacterial properties of titanium alkoxide/poplar wood composite prepared by sol-gel process. Mater. Lett. 89:101–103.

Rowell, R.M., LeVan-Green, S.L. Handbook of Wood Chemistry and Wood Composites. Taylor & Francis, New York, 2005.

Saka, S., Sasaki, M., Tanahashi, M. (1992) Wood-inorganic composites prepared by sol-gel processing I. Wood-inorganic composites with porous structure. Mokuzai Gakkaishi 38:1043–1049.

Saka, S., Ueno, T. (1997) Several SiO_2 wood-inorganic composites and their fire-resisting properties. Wood Sci. Technol. 31:457–466.

Shabir Mahr, M., Hübert, T., Schartel, B., Bahr, H., Sabel, M., Militz, H. (2012) Fire retardancy effects in single and double layered sol-gel derived TiO_2 and SiO_2-wood composites. J. Sol-Gel Sci. Technol. 64:452–464.

Tshabalala, M.A., Libert, R., Schaller, C.M. (2011) Photostability and moisture uptake properties of wood veneers coated with a combination of thin sol-gel films and light stabilizers. Holzforschung 65:215–220.

Tshabalala, M.A., Sung, L.-P. (2007) Wood surface modification by in-situ sol-gel deposition of hybrid inorganic-organic thin films. J. Coat. Technol. Res. 4:483–490.

Vuthaluru, H.B. (2004) Investigations into the pyrolytic behavior of coal/biomass blends using thermogravimetric analysis. Biores. Technol. 92:187–195.

Wang, X., Liu, J., Chai, Y. (2012) Thermal, mechanical, and moisture absorption properties of wood-TiO_2 composites prepared by a sol-gel process. Bioresources 7:893–901.

Yao, F., Wu, Q., Lei, Y., Guo, W., Xu, Y. (2008) Thermal decomposition kinetics of natural fibers: activation energy with dynamic thermogravimetric analysis. Polym. Degrad. Stabil. 93:90–98.

Zhang, X., Mu, J., Chu, D., Zhao, Y. (2016) Synthesis of fire retardants based on N and P and poly(sodium silicate-aluminum dihydrogen phosphate) (PSADP) and testing the flame-retardant properties of PSADP impregnated poplar wood. Holzforschung 70:341–350.